A Broadband Time-Varying Energy Maximising Control for Wave Energy Systems (LiTe-Con+): Framework and Experimental Assessment

A Broadband Time-Varying Energy Maximising Control for Wave Energy Systems (LiTe-Con+): Framework and Experimental Assessment

Demián García-Violini, Yerai Peña-Sanchez, Nicolás Faedo, Francesco Ferri, and John V. Ringwood, *Senior Member, IEEE*

***Abstract*—Motion of wave energy converters (WECs) is usually exaggerated as a consequence of the application of control strategies for energy absorption maximisation. With the aim of preserving the physical integrity of the devices, constraint handling mechanisms, as part of the underlying control strategies, are considered a key component. Recent developments in wave energy control include a linear time-invariant-based controller presented in the literature as LiTe-Con, which provides a simple constraint handling mechanism. However, this handling method can lead to conservative performance in certain scenarios. To overcome such limitations, this study presents a time-varying methodology for an online adaptation of the constraint handling mechanism in LiTe-Con, while preserving its original simplicity and efficiency. Experimental assessment of the presented control methodology is provided in this study, using a broad range of operating conditions. Results show that the presented control strategy (LiTe-Con+) exceeds the performance achievable with the original LiTe-Con. Additionally, the benefits of LiTe-Con+, such as low computational demand, technical versatility, and impressive performance level are highlighted.**

***Index Terms*—Wave energy, optimal control, impedance-matching, linear time invariant.**

Manuscript received 11 April 2022; revised 28 September 2022 and 26 November 2022; accepted 2 January 2023. Date of publication 16 January 2023; date of current version 21 June 2023. This work was supported in part by Science Foundation Ireland under Grant 13/IA/1886, in part by European Union's Horizon 2020 under Grant 731084, in part by Maynooth University under Grant 101024372, and in part by Politecnico di Torino. Paper no. TSTE-00368-2022. *(Corresponding author: Demián García-Violini.)*

Demián García-Violini is with the Dept. de Ciencia y Tecnología, CONICET and the Universidad Nacional de Quilmes, B1876BXD Buenos Aires, Argentina, and also with the Centre for Ocean Energy Research, National University of Ireland, W23 X021 Maynooth, County Kildare, Ireland (e-mail: ddgv83@gmail.com).

Yerai Peña-Sanchez is with the Euskal Herriko Unibertsitatea (EHU/UPV), Leioa, 48940 Bizkaia, España, and also with the Centre for Ocean Energy Research, National University of Ireland, W23 X021 Maynooth, County Kildare, Ireland (e-mail: yerai.p.17@gmail.com).

Nicolás Faedo is with the Marine Offshore Renewable Energy Lab., Department of Mechanical and Aerospace Engineering, Politecnico di Torino, 10129 Torino, Italy, and also with the Centre for Ocean Energy Research, National University of Ireland, W23 X021 Maynooth, County Kildare, Ireland (e-mail: nicolas.faedo@polito).

Francesco Ferri is with the Aalborg University, Thomas Manns Vej 23, 9220 Aalborg, Denmark (e-mail: ffer@build.aau.dk).

John V. Ringwood is with the Centre for Ocean Energy Research, National University of Ireland, W23 X021 Maynooth, County Kildare, Ireland (e-mail: john.ringwood@mu.ie).

Color versions of one or more figures in this article are available at https://doi.org/10.1109/TSTE.2023.3237023.

Digital Object Identifier 10.1109/TSTE.2023.3237023

I. Introduction

WAVE energy systems can play an important role in the global carbon neutrality goal, pledged to date by 110 countries [1]. With current global energy demand, which mainly depends on fossil fuels and projected to rise by 1% per year until 2040 [?], wave energy converters (WECs) can be key components in a carbon-free energy generation scheme, capable of satisfying global energy demand. However, due to existing technical and logistical challenges, WECs require further development to achieve cost-competitive power generation and, consequently, commercial viability [2].

Control technology plays a major part in the drive for economic viability of WECs. Throughout the wave energy literature, it is well-established that appropriate control technologies have the capability to enhance energy extraction from WECs. Such control strategies for WECs are generally categorised into two classes [3]: optimisation-based (OB) controllers and non-optimisation-based (nOB) controllers. Naturally, each methodology has its strengths and weaknesses [2]. Particularly, OB methodologies compute an optimal control input by solving an optimisation problem and can, therefore, deal with physical constraints obtaining (theoretically) optimal solutions [4]. Nonetheless, they require solution of a constrained optimisation problem at each controller sampling time, with a correspondingly large computational burden [?]. In general, OB strategies, which normally have the capability of handling constraints, include model predictive controllers [4], spectral/pseudospectral-based controllers [5], and moment-matching based controllers [6]. Particularly, OB strategies provide strict fulfilment of constraint requirements. On the other hand, nOB controllers appeal for their structural simplicity, which eases their design and implementation on virtually any hardware platform. However, such strategies either do not incorporate constraint handling mechanisms or those included are suboptimal [7]. In addition, in contrast to OB strategies, nOB controllers provide 'global and statistical' constraint handling, rather than hard constraint fulfilment.

Among the nOB strategies, to the best of the authors' knowledge, only the Simple & Effective (S&E) [8] controller and that presented in [?], referred to as LiTe-Con, provide intrinsic constraint handling mechanism, making them suitable for realistic operating environments [7]. However, the S&E controller requires an online instantaneous frequency estimation,

which is a challenging problem, particularly for polychromatic (broadband) sea-states [7]. In contrast, the LiTe-Con, experimentally validated in [9], only relies on linear time-invariant (LTI) dynamical structures and an estimate of the wave excitation force. The performance achievable by the LiTe-Con generally exceeds that obtained by the S&E controller [7], as shown in [?].

The constraint handling mechanism of the LiTe-Con [7] is based on a fixed gain adjustment of the control signal, which can be tuned using exhaustive simulation-based search. However, this constraint handling technique, which preserves the physical integrity of the device, can lead to conservative performance of the controller, compared to OB techniques [7]. In particular, an analysis related to energy maximisation *vs.* limit violation (motion restriction), is presented in [10] for the LiTe-Con, using a broad variation set for the constraint handling parameter, explicitly showing how different configurations can impact on the resulting performance. In addition, a comparison between unconstrained *vs.* constrained cases, for monochromatic and panchromatic sea-states, using a theoretical complex conjugate benchmark, is presented in [10], which cannot be performed in experimental conditions, due to the strict requirement for physical constraints in experimental settings and causality issues in complex conjugate control theory [7].

To improve the achievable performance of the LiTe-Con, this study presents a time-varying methodology for an online adaptation of its constraint handling mechanism. This methodology relies on real-time envelop estimation of the excitation force. Since the control structure presented in this paper is an upgraded version of the existing LiTe-Con, by means of a more effective constraint handle mechanism, it is referred to as LiTe-Con+. The technique used to estimate the excitation force envelop in real time is inspired by the Hilbert-Huang transform (HHT) [11]. To achieve more accurate envelop estimation, a set of future values of the excitation force can be also considered in the application of the HHT algorithm, which can be obtained using, for example, standard linear forecasting routines [?]. The LiTe-Con+ being a more effective, novel, and versatile time-varying energy maximising control framework, it preserves the original spirit of simplicity, and efficiency, of LiTe-Con. Experimental assessment of the LiTe-Con+ is provided, showing that it exceeds the performance achievable with LiTe-Con and standard passive controllers.

To summarise, the main contributions of the present study are listed below:

- A new energy-maximising control framework, with a novel time-varying approach to address motion constraints, is introduced, which:
  - –can effectively deal with narrow- or broad-banded sea states;
  - –is highly versatile in terms of real-time implementability on hardware platforms;
  - –shows encouraging performance levels;
- an algorithm for online envelope estimation is described;
- a complete experimental assessment is shown;
- an experimental comparison with existing control methodologies is presented, showing very satisfactory energy absorption levels.

The remainder of this paper is organised as follows. The fundamentals behind WEC modelling and energy maximising control of WECs are presented in Sections II-A and II-B, respectively, while Section III introduces the LiTe-Con+ controller. Experimental assessment of the LiTe-Con+ is demonstrated in Section IV and, finally, Section V encompasses the main conclusions of this study.

II. Energy Maximising Control in WEC Systems

In this section, the basics behind control-oriented WEC modelling are recalled (see for instance [12]), considering a single degree-of-freedom (DoF) WEC.

A. WEC Modelling

Using linear potential flow theory and Cummins' equation [13], the motion of a single DoF WEC can be described, for $t \in \mathbb{R}^+$, by

$$(m + m_\infty)\ddot{x}(t) = f_{\text{ex}}(t) - f_u(t) - k_{\text{h}}x(t) - h_{\text{r}} \star \dot{x}(t), \quad (1)$$

where the symbol $\star$ represents convolution, $x(t)$ is the device displacement, $f_{\text{ex}}(t)$ the wave excitation force, $f_{\text{h}}(t)$ the hydrostatic restoring force, $f_{\text{r}}(t)$ the radiation force, $m \in \mathbb{R}^+$ the mass of the device, $f_u(t)$ the control input applied by means of the power-take-off (PTO) system, k_{h} the hydrostatic stiffness, $h_{\text{r}}(t)$ the radiation impulse response function, and $m_\infty = \lim_{\omega\to+\infty} A_{\text{r}}(\omega)$. $A_{\text{r}}(\omega)$ and $B_{\text{r}}(\omega)$ are the so-called radiation added-mass and damping, respectively, defined from Ogilvie's relations [14] as

$$\begin{aligned} A_{\text{r}}(\omega) &= m_\infty - \frac{1}{\omega}\int_0^{+\infty} h_{\text{r}}(t)\sin(\omega t)dt, \\ B_{\text{r}}(\omega) &= \int_0^{+\infty} h_{\text{r}}(t)\cos(\omega t)dt. \end{aligned} \quad (2)$$

In (2) fully characterises the Fourier transform of $h_{\text{r}}(t)$, i.e.

$$H_{\text{r}}(\omega) = B_{\text{r}}(\omega) + \jmath\omega\left[A_{\text{r}}(\omega) - m_\infty\right], \quad (3)$$

where $h_r(t)$ and $H_r(\omega)$ denote a Fourier transform pair. Using (3), the model in (1) can be compactly expressed, in the frequency domain, as follows [12]:

$$V(\omega) = \frac{1}{Z_i(\omega)}\left[F_{\text{ex}}(\omega) - F_u(\omega)\right], \quad (4)$$

where

$$Z_i(\omega) = B_{\text{r}}(\omega) + \jmath\omega\left(m + A_{\text{r}}(\omega) - \frac{k_{\text{h}}}{\omega^2}\right). \quad (5)$$

Considering the force-to-velocity mapping in the Laplace domain:

$$G_0(s) = \frac{s}{s^2(m + m_\infty) + s\hat{H}_{\text{r}}(s) + k_{\text{h}}}\bigg|_{s=\jmath\omega} \approx \frac{1}{Z_i(\omega)}, \quad (6)$$

where $H_{\mathrm{r}}(\omega)$ is commonly computed using boundary-element methods, such as WAMIT [15], and $\hat{H}_{\mathrm{r}}(s) \approx H_{\mathrm{r}}(\omega)$, for $s = \jmath\omega$, with $\hat{H}_{\mathrm{r}}(s)$ a stable LTI system.

B. Optimal Control Condition

In WEC systems, the useful absorbed energy E, over the time interval $[0,\ T]$ with $T \in \mathbb{R}^+$, can be calculated as the integral of converted power

$$E = -\int_0^T \dot{x}(t) f_u(t) dt. \tag{7}$$

Considering the assumptions in Section II-A, the impedance-matching problem [12] allows the derivation of an optimal condition, in terms of $f_u(t)$ for maximum absorbed energy E in (7), in the frequency domain, as:

$$F_u(\omega) = -Z_i^\star(\omega) V(\omega), \tag{8}$$

where $Z^\star(\omega)$ denotes the complex conjugate of $Z(\omega)$. The optimal condition, defined in (8), can be alternatively expressed in terms of an optimal velocity profile $V^{opt}(\omega)$, with a purely real mapping, as:

$$V^{opt}(\omega) = \frac{1}{Z_i(\omega) + Z_i^\star(\omega)} F_{\mathrm{ex}}(\omega) = \frac{1}{2B_{\mathrm{r}}(\omega)} F_{\mathrm{ex}}(\omega), \tag{9}$$

which defines a zero-phase-locking condition between the device velocity and $f_{\mathrm{ex}}(t)$, often considered as a control performance indicator [?]. (8) and (9) define the well-established impedance-matching condition [12], which can be rewritten in a control form as $H_{fb}(\omega) = Z_i^\star(\omega)$. This condition represents a feedback (FB) control structure, with the controller $H_{fb}(\omega)$ in the feedback path [?]. Even though its solution is a standard result in the WEC control literature, the intrinsic non-causality of $H_{fb}(\omega)$ does not allow for practical implementation of the controller (see [?] for a detailed discussion).

Considering such an impedance-matching condition, both the system $G_0(s)$ and the controller $H_{fb}(s)$ can be described in the frequency-domain as:[1]

$$G_0(s)\Big|_{s=\jmath\omega} = \mathbb{Re}(G) + \jmath\mathbb{Im}(G), \tag{10}$$

$$H_{fb}(s)\Big|_{s=\jmath\omega} = \frac{1}{\mathbb{Re}(G) - \jmath\mathbb{Im}(G)}. \tag{11}$$

Then, the optimal mapping from $F_{\mathrm{ex}}(\omega)$ to $V^{opt}(\omega)$, described in (9), can be equivalently expressed as:

$$\frac{V^{opt}(\omega)}{F_{\mathrm{ex}}(\omega)} = T^{opt}_{f_{\mathrm{ex}} \to v}(\omega) = \frac{\mathbb{Re}(G)^2 + \mathbb{Im}(G)^2}{2\mathbb{Re}(G)}. \tag{12}$$

III. Time-Varying Control Approach: LiTe-Con+

This section outlines the proposed LiTe-Con+ control strategy for WECs. To this end, Section III-A recalls the basics of the LiTe-Con [?]. Then, the design procedure of the LiTe-Con+ is described in Section III-B.

[1]For the sake of simplicity of notation, let $\mathbb{Re}(G) = \mathbb{Re}\{G_0(\jmath\omega)\}$ and $\mathbb{Im}(G) = \mathbb{Im}\{G_0(\jmath\omega)\}$ denote the *real-part* and *imaginary-part* operators, respectively.

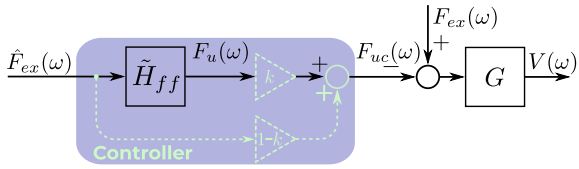

Fig. 1. Force-to-velocity scheme. The purple box indicates the control structure including the constraint handling mechanism.

A. Lite-Con

The optimal control condition for the mapping from $F_{\mathrm{ex}}(\omega)$ to $V(\omega)$, expressed in (12), can be equivalently obtained using a feed-forward (FF) control structure, as follows

$$H_{\mathrm{ff}}(\omega) = \frac{\mathbb{Re}(G) + \jmath\mathbb{Im}(G)}{2\mathbb{Re}(G)}, \tag{13}$$

where the FF mapping $H_{\mathrm{ff}}(\omega)$ is equivalent to the FB structure $H_{\mathrm{fb}}(\omega)$, indicated in (11) [?]. Thus, $F_u(\omega) = H_{\mathrm{ff}}(\omega) F_{\mathrm{ex}}(\omega)$.

Using frequency-domain system identification algorithms [16], the LiTe-Con approximates $H_{\mathrm{ff}}(\jmath\omega)$ with a LTI-stable and implementable dynamical system $\tilde{H}_{\mathrm{ff}}(s)$, i.e.:

$$\tilde{H}_{\mathrm{ff}}(s)\Big|_{s=\jmath\omega} \approx H_{\mathrm{ff}}(\omega). \tag{14}$$

The LiTe-Con proposes a constraint handling mechanism, using a constant $k \in [0,\ 1]$, so that the control force $F_u(\omega)$ is modified as:

$$F_{uc}(\omega) = \left[k\tilde{H}_{\mathrm{ff}}(\omega) + (1-k)\right] \hat{F}_{\mathrm{ex}}(\omega), \tag{15}$$

where $\hat{F}_{\mathrm{ex}}(\omega)$ is an estimate of $F_{\mathrm{ex}}(\omega)$. It is straightforward to check that $F_{uc}(\omega) = F_u(\omega)$, when $k = 1$.

The block diagram of the resulting force-to-velocity scheme of the LiTe-Con, as indicated in (15), is shown in Fig. 1, in which the constraint handling mechanism of the LiTe-Con is highlighted with a highlighted path.

From (15), if $k = 1$, the controller matches the optimal expression in (12) while, if $k = 0$, the resulting force-to-velocity mapping is set to zero, blocking the device motion (assuming ideal $f_{\mathrm{ex}}(t)$ estimation). This constraint handling methodology restricts the device motion, which is important in minimising the risk of component damage while, at the same time, preserves the zero-phase-locking between velocity and $f_{\mathrm{ex}}(t)$ (see (9)), arising from the energy maximising control. To determine a value of k that fulfils the control design specifications (absorbed power *vs.* operational range), an exhaustive simulation procedure is generally required. Since the aim is to prevent any excessive motion in a worst-case scenario, it can lead to over-conservative performance of the LiTe-Con controller.

B. Lite-Con+

To extend the range of achievable performance of the LiTe-Con presented in Section III-A, a time-varying modulation mechanism for the constraint handling value k is introduced. A proposed k-modulation strategy uses information available in the estimated $f_{\mathrm{ex}}(t)$, specifically its instantaneous envelop, to

restrict or release the control action. It is important to note that the use of WEC motion for the adaptation of k would create a new closed-loop system, for which guaranteeing stability represents a challenging nonlinear control problem. In contrast, the use of $f_{\text{ex}}(t)$ to modulate the gain value k entirely decouples the constraint handling mechanism from the WEC motion, at least under the linear assumptions considered in Section II-A. Decoupling k and the device motion significantly simplifies both the constraint handling and control problems, mainly in terms of stability while, at the same time, allows for an efficient use of the operational range. It should be noted that this methodology does not provide fully optimal constraint handling, i.e. in a constrained optimal control sense [4]. However, it significantly improves the performance generated with the LiTe-Con, as will be shown in Section IV.

1) Wave Excitation Force Envelop Estimation: The envelop estimation methodology considered for this study is inspired by the HHT approach applied in, for example, the control strategy of [17]. Generally, the application of the HHT assumes non-stationary signals that can be approximately described by

$$x(t) = \mathbb{R}\mathrm{e}\left\{\sum_{i=1}^{N} \hat{E}_i(t) e^{\jmath \int \hat{\omega}_i(t) dt}\right\}, \tag{16}$$

where $\hat{E}_i(t)$ and $\hat{\omega}_i(t)$ represent the instantaneous amplitude and frequency of the i-th individual component. The framework introduced by the HHT is useful for the treatment of signals in the wave energy field, due to their oscillatory nature. In particular, $f_{\text{ex}}(t)$ can be considered as a quasi-periodic single-frequency non-stationary process [8], as follows

$$f_{\text{ex}}(t) \approx \hat{E}(t) \cos\left(\int \omega_{\text{ex}}(t) dt\right), \tag{17}$$

where $\hat{E}(t)$ and $\omega_{\text{ex}}(t)$ represent the instantaneous envelop and frequency of $f_{\text{ex}}(t)$, respectively. Generally, instantaneous frequency estimation in general non-stationary processes [11], as presented in [18] for a control application in WEC systems, is considered a challenging problem [?] while, in some applications, it has little meaning. Conversely, instantaneous envelop estimation in quasi-periodic non-stationary processes, as required for the LiTe-Con+, is a well-defined problem and several algorithms have been proposed in the literature [11].

The envelop estimation approach considered in this study is based on interpolation of the local maxima of $|f_{\text{ex}}(t)|$ contained in a time-window of length W_T, defined using current and past values of the excitation force, although it could include future (predicted) values of the excitation force to improve the obtained results. Thus, the time-windows of past and predicted values have lengths W_p and W_f, respectively, i.e. $W_T = W_p + W_f$. The window lengths W_p and W_f are related to the shift registers F_p and F_f, respectively, required for the implementation of the algorithm. The main definitions required for the implementation of the envelop estimation routine presented in this study are indicated in Fig. 2, where the set of local maxima P_k in the total time-window, $f_{\text{ex}}(t)$ and its absolute value ($|f_{\text{ex}}(t)|$), the current time (t_0), and the envelop estimation ($\hat{E}(t_0)$), are shown.

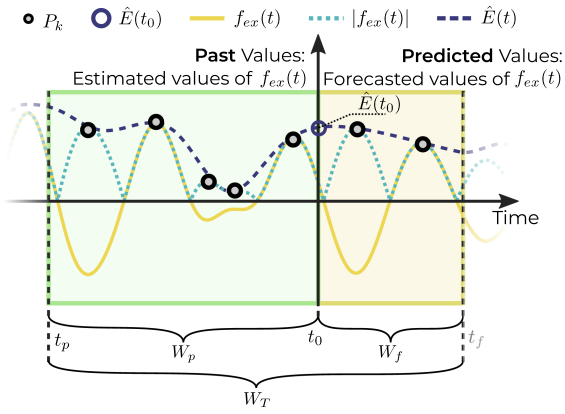

Fig. 2. Envelop estimation procedure.

Note that, for representation purposes, the actual continuous-time $f_{\text{ex}}(t)$ and its absolute value are shown in Fig. 2 while, in the implementation of the algorithm, the data are considered in discrete time, using a sampling period T_m. Additionally, the data related to past excitation force values are obtained from an $f_{\text{ex}}(t)$ estimation routine (and therefore denoted as $\hat{f}_{\text{ex}}(t)$), i.e. $\mathrm{F}_p = [\hat{f}_{\text{ex}}(t_p),\ \hat{f}_{\text{ex}}(t_p + T_m),\ \ldots,\ \hat{f}_{\text{ex}}(t_0)]$ with $t \in [t_p,\ t_0]$. Equivalently, the data related to W_f, i.e. $\mathrm{F}_f = [\hat{f}_{\text{ex}}(t_0),\ \tilde{f}_{\text{ex}}(t_0 + T_m),\ \ldots,\ \tilde{f}_{\text{ex}}(t_f)]$ with $t \in [t_0,\ t_f]$, are obtained from a $f_{\text{ex}}(t)$ forecaster (denoted as $\tilde{f}_{\text{ex}}(t)$). The final implementation of the procedure is carried out using a receding horizon scheme. Thus, to obtain an estimate of the envelop of $f_{\text{ex}}(t_0)$, the algorithm considered for this study interpolates the set of local maxima $\{\mathrm{P}_k\}$ contained in the total time-window where, eventually, the data related to W_f could be an empty set (no foretasted data considered). The general application of the envelop estimation procedure is detailed in Algorithm 1.

Algorithm 1: Envelop Estimation (**Alg1**).

Input: W_p,W_f,$\hat{f}_{\text{ex}}(t_0)$
Output: $E(t_0)$
Current time t_0
while $t_0 > W_p$ **do**
  (i) $t_p \leftarrow t_0 - W_p$;
  $\mathrm{F}_p \leftarrow \left[\hat{f}_{\text{ex}}(t_p),\ \hat{f}_{\text{ex}}(t_p + T_m),\ \ldots,\ \hat{f}_{\text{ex}}(t_0)\right]$;
  if *is a future estimation considered?* **then**
    $\left\{\tilde{f}_{\text{ex}}(t_0 + T_m),\ \ldots,\ \tilde{f}_{\text{ex}}(t_f)\right\} \leftarrow$ prediction $f_{\text{ex}}(t)$ for $t \in [t_0 + T_m,\ t_f]$
    $\mathrm{F}_f \leftarrow \left[\hat{f}_{\text{ex}}(t_0),\ \tilde{f}_{\text{ex}}(t_0 + T_m),\ \ldots,\ \tilde{f}_{\text{ex}}(t_f)\right]$;
  else
    $\mathrm{F}_f \leftarrow \emptyset$
  $\mathrm{F}_T \leftarrow [\mathrm{F}_p,\ \mathrm{F}_f]$
  $\{\mathrm{P}_k\} \leftarrow$ Identify the local maxima in $|F_T|$
  $E(t) \leftarrow$ Interpolate the values in the set $\{\mathrm{P}_k\}$
  $E(t_0)$ is computed as outcome
  return to (i)

1) Practical Notes:

i) *Window lengths:* It is recommended to define W_p and W_f as (at least) twice and once the typical period of the considered sea state (SS), respectively, i.e. $W_p \geq T_{SS}$ and

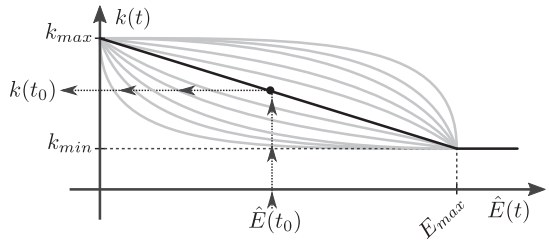

Fig. 3. Different possibilities for the mapping $\mathcal{K}$ required for envelop computation.

$W_f \geq T_{SS}$, with T_{SS} the typical period of a particular sea state. This guarantees, from a statistical perspective, the existence of sufficient elements in $\{\mathrm{P}_k\}$ to effectively perform the interpolation. The length of the time window must be designed to guarantee sufficient peaks in $|f_{ex}(t)|$ to effectively estimate the envelop, at least two peaks. If the length of the time window approaches zero, then the algorithm cannot be effectively implemented, since the interpolation can not be successfully performed.

ii) *Window initialisation:* Both F_p and F_f can be initialised using, for instance, uniform random until both shift registers are completely filled. This procedure does not significantly affect the overall performance, since it only influences the initial period of time.

iii) *Peak interpolation:* For the peak interpolation stage, there are several approaches that are usually considered for the application of the HHT [?], such as cubic spline interpolation, which is used in this study, although other interpolation methodologies can be alternatively considered.

iv) *Empty peak set:* In the case of obtaining a set with no maximum values, the envelop estimates from the previous iteration can be utilised.

2) $k(t)$-Modulation: To obtain the required modulation of the value k, a strictly decreasing mapping $\mathcal{K}: \mathbb{R}^+ \mapsto [k_{\min}, k_{\max}]$, which transforms the estimated envelop into the resulting k-gain modulation, is required. To this end, at least three tuning parameters are required: an estimate of the expected maximum value of the envelop $E_{\max}$, and the interval limits for the modulation of $k(t)$, defined as the constant values $k_{\min}$ and $k_{\max}$. Thus, the mapping $\mathcal{K}$ can be defined as shown in Fig. 3, where a linear mapping is shown using a black line, while a set of alternative $k(t)$ are depicted using grey lines. It is worth mentioning that different mappings can be designed and selected, even beyond the cases illustrated in Fig. 3. In particular, considering a selection among the example curves illustrated in Fig. 3, this family of curves provides the capability of *'compression'* or *'decompression'*, where the linear mapping represents the limit case between the upper and lower set of curves. By way of example, the upper set of curves in Fig. 3 (above the linear mapping) provides more relaxed constraint handling (decompression). Conversely, the lower set of curves (in Fig. 3 below the linear mapping) provides more aggressive constraint handling (compression). In particular, the linear mapping, illustrated with a black line in Fig. 3 and considered in the application case of Section IV, provides a balanced and gradual (linear) transition between $k_{\min}$ and $k_{\max}$, requiring only a small number of defining parameters.

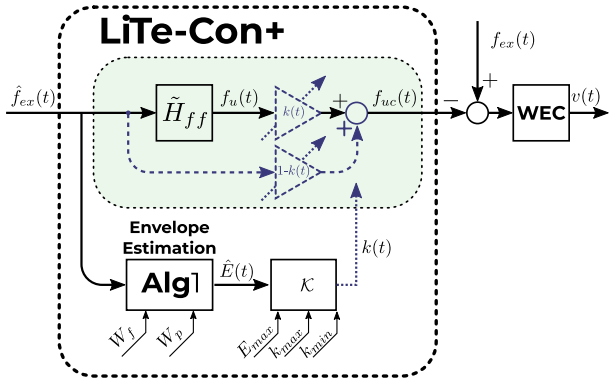

Fig. 4. Block diagram of the LiTe-Con+.

In particular, taking into account the linear mapping considered in this study, the resulting relationship between $\hat{E}(t)$ and $k(t)$ is,

$$\mathcal{K}: k(t) = \begin{cases} \left(\frac{k_{\min}-k_{\max}}{E_{\max}}\right)\hat{E}(t) + k_{\max} & \text{if} \quad 0 \leq \hat{E}(t) \leq E_{\max} \\ k_{\min} & \text{if} \quad \hat{E}(t) > E_{\max} \end{cases}. \tag{18}$$

The block diagram of the resulting force-to-velocity relationship, for the LiTe-Con+, is shown in Fig. 4.

It is important to remark that the presented approach requires more tuning parameters than the LiTe-Con. However, to define such parameters (namely $E_{\max}$, $k_{\min}$, and $k_{\max}$), an exhaustive simulation-based search can be used, similar to the procedure introduced to obtain the static k value in the LiTe-Con. Therefore, the tuning process is, methodologically and in terms of complexity, similar to the tuning process required for the LiTe-Con. The general design procedure required for the LiTe-Con+ is outlined below:

1) Considering the WEC system, obtain the optimal energy maximising condition defined in (12).
2) Obtain the LTI approximation $\tilde{H}_{\mathrm{ff}}(s)$, defined in (14).
3) Define an envelope estimation algorithm.
4) Define a modulation profile $\mathcal{K}$.
5) Apply the control structure indicated in Fig. 4.

It must be noted that the set of curves illustrated in Fig. 3 only aims to exemplify a general family of possible mappings. In general, the mapping $\mathcal{K}$ is not restricted to the family illustrated in Fig. 3, and the only restrictions on $\mathcal{K}$ are that it must be: i) strictly decreasing, and ii) continuous. Beyond requirements i) and ii), there are no restrictions on the definition of $\mathcal{K}$. In particular, the selection of a linear mapping preserves and emphasises the spirit of simplicity of the presented method and its predecessor, the LiTe-Con. Additionally, tuning of a linear mapping $\mathcal{K}$ requires only the calibration of a small number

TABLE I
DIMENSIONS, RELATIVE TO THE STILL WATER LEVEL (SWL), AND MASS PROPERTIES FOR THE 1/20TH SCALE WAVESTAR DEVICE

Parameter	Value	[Unit]
Float Mass	3.075	[kg]
Float MoI (at C_g)	0.001450	[kg·m^2]
Float Draft	0.11	[m]
Float Diameter (at SWL)	0.256	[m]
Arm Mass	1.157	[kg]
Arm MoI (at C_g)	0.0606	[kg·m^2]

of parameters, which simplifies tuning effort. It can also be mentioned that $\mathcal{K}$ could be tuned using a theoretically-based method, such as an optimisation routine and optimality criterion [?]. However, this approach is beyond the scope of this study, since this methodology is not aligned with the essence of simplicity of the presented control strategy. It is worth noting that, even using an empirically-based tuning method with a linear mapping $\mathcal{K}$, the considered LiTe-Con+ significantly outperforms its predecessor, the LiTe-Con, as experimentally shown in Section IV.

A general rule, for calibration of the mapping $\mathcal{K}$, as required by the item 4) in the design procedure listed before, can be described in terms of the fixed parameters $k_{\min}$ and $k_{\max}$, both required for any mapping $\mathcal{K}$. In particular, if the wave excitation force presents large force values (or sudden peaks), then a low value for $k_{\min}$ (close to zero) can prevent a collision with the constraints limits. Analogously, for a wave excitation force with a reduced dynamic range, with its corresponding envelope estimation, a large value of $k_{\max}$ (close to one) fully exploits the complete operational dynamic range. It is worth noting that a general mapping $\mathcal{K}$, as for example illustrated with grey lines in Fig. 3, requires additional tuning parameters, compared to a linear mapping, and an improvement in performance cannot be generally guaranteed.

IV. EXPERIMENTAL ASSESSMENT

An experimental campaign, using LiTe-Con+, was carried out in the wave basin at Aalborg University. The employed prototype is a 1/20th scale model of a single float of the Wavestar WEC. The relevant dimensions and mechanical properties of the system are listed in Table I.

A photograph and the schematic of the prototype system used for the experimental assessment are shown in Fig. 5(a) and (b), respectively. Note that the experimental infrastructure used for the assessment of the LiTe-Con+ is the same that used for the experimental validation of the LiTe-Con in [9], and previously detailed in [?]. Data acquisition is implemented using a rapid control prototyping hardware architecture, with the controller implemented in real-time using Matlab/Simulink (version 2016b). For the sake of brevity, the interested reader is referred to [9] for a detailed description of the complete experimental setup, including the WEC prototype, sensing and actuation systems, hardware computer and acquisition, wave basin dimensions, etc. In addition, a detailed multimedia description of the experimental system, particularly the system identification methodology described in Section IV-A, can be found in [?], which includes photographs and videos. It must be noted that this study does not consider electrical issues, such as electromechanical conversion, power losses, PTO efficiency, etc. The presented study focusses on the first step of the energy absorption chain, i.e. the efficiency in the conversion from power available in waves into mechanical power.

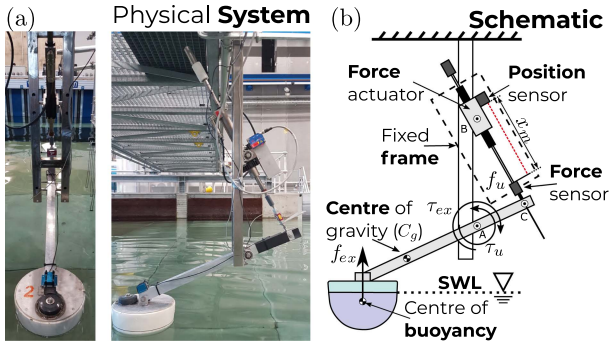

Fig. 5. (a) Photograph and (b) schematic of the WEC system.

A. System Characterisation and LiTe-Con+ Design

1) System Characterisation: The WEC model, expressed in (10) and used for control design, is obtained following the *black-box* system characterisation methodology presented in [9]. Thus, in the total absence of waves, a set of chirp signals, with amplitudes contained in the set $\mathcal{A} = \{2.5, 5, 7.5, \ldots, 17.5, 20\}$ N and a duration of 140 seconds, is applied through the force actuator, depicted in Fig 5(b), to obtain a dynamical characterisation of the WEC prototype. Each chirp signal is defined as a linear frequency sweep with range $[0.1, 60]$ rad/s, covering the resonance frequency of the system, with a decade below and above. Unlike [9], the system ID experiments are performed considering down-chirp signals, placing the low frequencies at the end of the experiment, to reduce wave reflections from the walls of the basin (shorter waves travel more slowly). Furthermore, in this study, the system model is considered from torque to angular motion, in contrast to [9], where the system is considered from force to linear motion. The force-to-torque transformation can be obtained with standard geometric and trigonometric tools, considering the dimensions in Table I and the schematic in Fig. 5(b). For characterisation of the system, the chirp forces are applied to the WEC system, obtaining a set of inputs (excitation torque), $\tau_{\text{ex}}^i(t)$, and outputs (angular velocity), $\dot{\theta}^i(t)$, with $i = 1, 2, \ldots, 8$ correspondingly to each element in $\mathcal{A}$. Then, this set of input-output pairs is used to define an empirical transfer function estimate (ETFE) which, using a subspace system identification algorithm [19] and a subsequent passivasation technique [?], is used to generate a LTI nominal representation of the torque-to-angular velocity mapping, $G_0(j\omega)$, depicted in Fig. 6. Further details on the system ID scheme can be found in [9].

2) LiTe-Con+ Design: To obtain the LTI system $\tilde{H}_{\text{ff}}(s)$, as indicated in (14), the design guidelines in [?] and [9] for the LiTe-Con are considered in this study. Using the experimental characterisation and the nominal WEC description $G_0(s)$, the

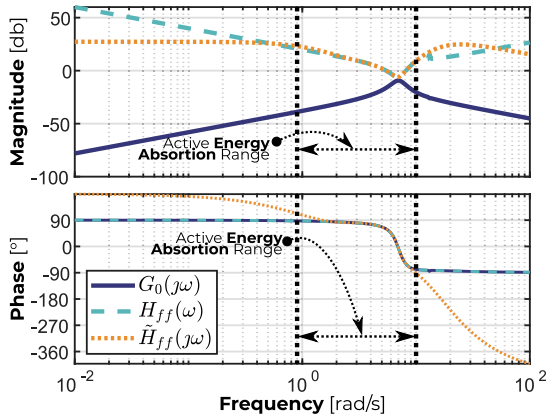

Fig. 6. Frequency responses of $G_0(s)$, $H_{\text{ff}}(\omega)$, and $\tilde{H}_{\text{ff}}(\jmath\omega)$.

TABLE II
H_s AND T_p OF THE CONSIDERED SSS

Sea State	H_s [m]	T_p [s]
SS1	0.0520	1.836
SS2	0.1042	1.836
SS3	0.0625	1.412
SS4	0.1042	1.412

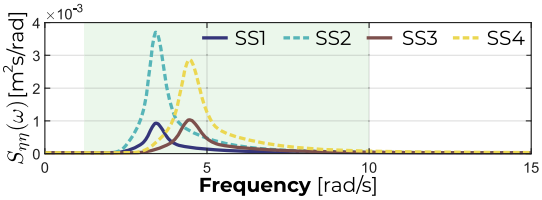

Fig. 7. Spectral power density of the considered SSs.

LTI structure $\tilde{H}_{\text{ff}}(s)$ is obtained considering the expressions in Equations (13)–(15). The structure $\tilde{H}_{\text{ff}}(s)$ is computed using a moment-matching-based system identification approach, proposed in [16], using four matching points, obtaining, therefore, a eighth-order LTI stable system $\tilde{H}_{\text{ff}}(s)$. The frequency responses of both $H_{\text{ff}}(\omega)$ and $\tilde{H}_{\text{ff}}(\jmath\omega)$ are shown in Fig. 6. Note that the area indicated and highlighted with a dashed double-side arrow in Fig. 6, between $[0.9,\ 10]$ rad/s, indicates the active energy absorption range considered in this study, as described in (14), according with the operation conditions defined by the SSs introduced in Section IV-B.

B. Sea States

Inspired by the experimental cases in [9], four different irregular SSs (SS1-SS4), generated from a JONSWAP spectral density function with peak shape parameter $\gamma = 3.3$ [20], are considered for the experimental assessment. The significant wave heights H_s, and peak periods T_p, are listed in Table II.

Fig. 7 shows the energy content of the three SSs by means of their power spectral density, denoted by $S_{\eta\eta}^{1-4}(\omega)$ for SS1-SS4, respectively. The shadowed area in Fig. 7 indicates the range considered in this study to optimise, as described in Section IV-A2 (Fig. 6), energy absorption.

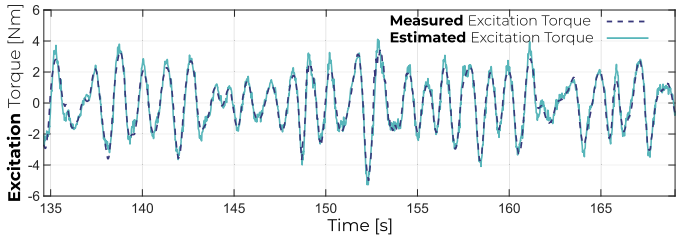

Fig. 8. Measured and estimated $\tau_{\text{ex}}(t)$ for SS4.

C. Excitation Torque Estimation

Knowledge of current excitation torque is required for the implementation of the LiTe-Con+. Since the excitation torque ($\hat{\tau}_{\text{ex}}(t)$) is an unmeasurable quantity for the moving WEC case, it has to be estimated based on other (measurable) quantities. The estimation strategy considered for this analysis estimates $\hat{\tau}_{\text{ex}}(t)$ using only measurements from the position sensor on the WEC prototype (see Fig. 5(b)). The estimation strategy is based on a Kalman filter, as described in [9].

To assess the performance of the torque estimator, a reference value for the 'actual' $\tau_{\text{ex}}(t)$ is required. To this end, a $\tau_{\text{ex}}(t)$ reference is defined following the fixed-body methodology adopted in [9]. The set of waves described in Table II are generated in the wave tank, with the device fixed in its equilibrium position. Since the device is not moving, radiation and hydrostatic forces are zero, so that the total force measured on the device using the force sensor is exactly $f_{\text{ex}}(t)$, or its geometrically equivalent torque $\tau_{\text{ex}}(t)$. By way of example, a comparison between the measured and estimated $\tau_{\text{ex}}(t)$, for SS4, is shown in Fig. 8. As reported in [9], due to the existing noise level in the position measurements, the obtained torque estimates are more noisy than the raw measurements obtained during fixed-body experiments.

D. Experimental Envelop Estimation and $k(t)-$modulation

To obtain an envelop estimate, Algorithm 1 is applied. Thus, the required parameters W_p and W_f have been set to $2T_p$ and T_p, respectively, and therefore change for each SS. To obtain a maximum experimental performance benchmark of the LiTe-Con+, the modulation of $k(t)$ is computed for the presented performance assessment study in a earlier preprocessing stage, using the torque signals acquired with the fixed-body experiments. Thus, without loss of generality, this process isolates the selected k-modulation methodology from the control problem, while a general performance perspective is provided. Fig. 9(a) shows the results of the estimated envelop obtained for SS4.

From the results shown in Fig. 9(a), it can be seen that the envelop estimation algorithm provides, in general, acceptable performance. For the sake of brevity, only the results of the envelop estimation for SS4 are shown, but similar results are obtained for SS1-SS3. Additionally, it is worth highlighting that, even though the algorithm performance can temporarily

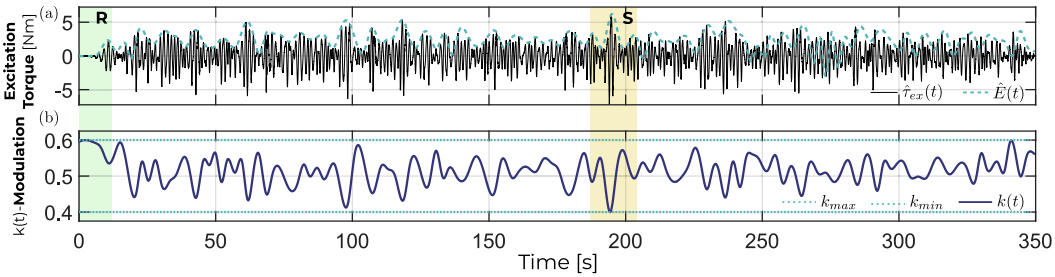

Fig. 9. (a) Envelop estimation of the wave excitation torque for SS4. (b) Resulting modulation of $k(t)$ for SS4.

drop due to noise or high-frequency oscillations in the estimated excitation torque, as for example shown in Fig. 9 at $t = 275$ s, the obtained envelop estimate is adequate for the control purpose pursued in this study.

Following Algorithm 1, to get the final modulation of $k(t)$, a linear transformation $\mathcal{K}$ is considered. Thus, in this study, $k_{\min}$ and $k_{\max}$ are set to 0.4 and 0.6, respectively, and $E_{\max} = \max\{\tau_{\text{ex}}^i(t)\}$, where $\tau_{\text{ex}}^i(t)$, with $i \in \{1, 2, 3, 4\}$ indicating the SS, is the measured $\tau_{\text{ex}}(t)$ obtained for the particular realisation of the $i-$th SS using the fixed-body experiment, as discussed in Section IV-C. Note that, in a realistic implementation, $E_{\max}$ can be precisely approximated using an exhaustive simulation methodology. Fig. 9(b) shows the results of the $k(t)-$modulation obtained for SS4 during a control experiment. As in Fig. 9(a), only the results for SS4 are shown, but the results for the other SSs are similar.

Two areas have been highlighted using green ($t \in [0, 15]$ s) and yellow ($t \in [188, 205]$ s) in Fig. 9, denoted as **R** and **S**, respectively. These highlighted events show both extremes of the presented constraint handling approach. In **R**, $\tau_{\text{ex}}(t)$ is close to zero and, consequently, $k(t)$ is virtually at $k_{\max}$. Conversely, in **S** $\tau_{\text{ex}}(t)$ achieves its maximum and $k(t)$ is close to $k_{\min}$. Thus, the events **R** and **S** in Fig. 9 illustrate the dynamic constraint handling performance LiTe-Con+.

To assess the control performance, two realisations of each SS are considered in this study. In addition, to establish a performance reference, the results are compared to those obtained using two additional existing control methodologies: the LiTe-Con and a passive (proportional) control. Since the LiTe-Con has been already compared to different control methodologies in the literature (see, for example, [3] and [?]), this new comparison provides a clear general perspective of the performance achieved by the LiTe-Con+. The same LTI structure $\tilde{H}_{\text{ff}}(s)$, is applied for both the LiTe-Con+ and LiTe-Con, setting a constant k gain for the LiTe-Con of 0.6 and 0.4 for SS1-SS3 and SS2-SS4, respectively. The passive controller, a widely considered standard approach [9], is defined as:

$$\tau_u^i(s) = k_P^i \dot{\theta}(s), \tag{19}$$

where $i \in \{1, 2, 3, 4\}$ indicates the SS. Thus, k_P^i is specifically designed for each SS to maximise the absorbed energy while preserving a safe operational range. Note that, while the same LiTe-Con+ tuning is used for all the cases, designed to address with one structure SS1-SS4, both passive and LiTe-Con schemes are specifically designed for each SS, which is less convenient

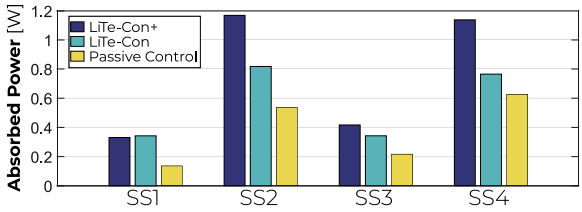

Fig. 10. Average power obtained for sea states 1-4.

for the LiTe-Con+. However, the LiTe-Con+ significantly exceeds the performance obtained with the other controllers, as shown in the following subsections. It is worth mentioning that this study does not compare the presented control methodology with optimisation-based strategies. Such comparison can be inferred by contrasting the results in [?] and those in this section. A study using the same experimental setting but with an optimisation-based controller will be subject of future research. It must be noted that the suggested benchmarking, considering a LiTe-Con and a set of passive controllers, is based on two considerations. Firstly, the LiTe-Con has been previously compared with different control strategies in, for example, [3], [?] and [?], using optimisation- and non-optimisation-based control schemes, including proportional-integral (PI) controllers, spectral- and moment-matching-based controllers, and theory-based complex-conjugate controllers (covering the complete bandwidth), for both constrained and unconstrained cases. Secondly, passive and PI controllers can only provide narrowband absorption capacity, in contrast to LiTe-Con which, by definition, provides a broadband energy maximising control solution extending, in the spectral domain, the energy absorption performance. Thus, the suggested comparative assessment provides a clear level playing field to analyse the performance of LiTe-Con+. Finally, to asses the control performance in a constrained experimental setting, the motion range is restricted to $\pm 20°$, which guarantees a safe operating range.

1) Absorbed Energy: To assess the performance in terms of absorbed power, the average absorbed power (see (7)), obtained with each realisation, for each SS, is shown in Fig. 10. It is clear that the performance of the LiTe-Con+ is generally always greater than the performance for the other control structures.

It can be noted that, for SS1, both the LiTe-Con and the LiTe-Con+ provides, in terms of absorbed power, virtually the same level of performance, due to the relative inactivity of the constraint handling mechanisms. In contrast, for SS2 and SS4,

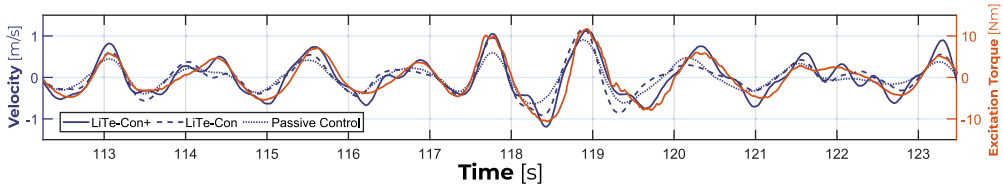

Fig. 11. Velocities obtained with different controllers and the wave excitation torque for SS4.

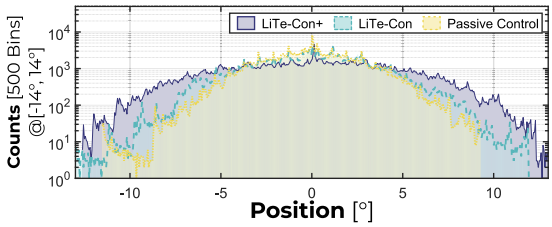

Fig. 12. Dynamic range analysis for each controller. A histogram for the range $[-14°, 14°]$ with 500 bins is considered.

which represent the largest considered SSs in terms of power spectral density, the LiTe-Con+ obtains a significant improvement of 42.87% and 48.68%, respectively, while, for SS2, with a lower power spectral density, the improvement is 21.71%. Thus, it is clear that the larger the demanded operative range (where constraint handling becomes more active), generated by more energetic SSs, the greater the benefit of the LiTe-Con+. Note that the performance obtained using the LiTe-Con+ for SS1 could be improved using a more specific set of tuning parameters for the mapping $\mathcal{K}$, optimised for SS1, which is not the case for the LiTe-Con, where the constant k is specifically determined for each SS, as previously mentioned.

2) Time Domain and Dynamical Range: The improved results obtained by the LiTe-Con+ are a consequence of a better use of the dynamic range of the WEC system. By way of example, Fig. 12 shows, for SS4, the resulting operational range of each control strategy, using a histogram in the range $[-14°, 14°]$ with 500 bins, counting the number of occurrences within each bin. Thus, Fig. 12 analyses, sample by sample, the number of occurrences inside each bin, and provides a comprehensive assessment on the dynamical (motion) distribution over the operational dynamic range (within the constraints). It can be seen that the operational range achieved by the LiTe-Con+ is significantly larger than that achieved by the LiTe-Con, and the passive controller. It must be noted that, among the considered sea-states, SS2 represents the most energetic and, consequently, motion-demanding, sea-state. As a result, SS2 has been mainly considered in the tuning process of the LiTe-Con+ in this study. To strictly fulfil the required set of constraints, either an optimisation-based controller should be considered, or a LiTe-Con+ must particularity tuned for a specific sea-state.

Similarly, considering the control performance analysed in the time domain, a comparison between the system velocity and $\tau_{\text{ex}}(t)$, for each control strategy, is shown in Fig. 11. As indicated in (12), under the optimal condition for power generation, WEC velocity and excitation torque (force) must show phase alignment. From Fig. 11, it is clear that the velocity generated with the LiTe-Con+ achieves the best phase agreement with $\tau_{\text{ex}}(t)$.

It should be also noted that, although this study does not directly cover time-varying sea-states, four markedly different sea-states have been analysed in this study. Thus, considering the fact that the parameters of the controller have not changed with the sea-states, it can reasonably be assumed that the performance of the controller would not be affected in a scenario with a time-varying sea-state. It is important to note that the requirement for constraint handling is not explicitly shown in this study. Nonetheless, if the constraint handling mechanism could be relaxed (or even removed), due to the existence of an additional motion margin, the control system would be able to absorb more energy, which is the main objective of the LiTe-Con+. However, if there were no constraint handling mechanism, attempts could be made to exceed the physical/operational system limits, resulting in potential system damage, or failure.

V. Conclusion

The present study introduces a new energy-maximising time-varying framework for wave energy control. The control approach uses the foundations considered for the LiTe-Con framework, and includes a novel time-varying constraint handling mechanism to improve the resulting operating range and, hence, absorbed energy. From a general perspective, the control framework presented in this study is a versatile approach that can address a broad range of operating conditions. From the experimental results, it is shown that the presented control approach, LiTe-Con+, is more efficient than its predecessor, the LiTe-Con. Also, regarding the experimental assessment, this study shows that, with a linear mapping $\mathcal{K}$, the controller can be straightforwardly tuned, achieving a very acceptable level of performance. Thus, the presented control approach is suitable for implementation in realistic applications, due to its simplicity and low computational requirements. Summarising, the LiTe-Con+ offers an appealing balance between simplicity and energy-maximising performance, convenient for realistic WEC applications.

References

[1] B. Guo and J. V. Ringwood, "A review of wave energy technology from a research and commercial perspective," *IET Renewable Power Gener.*, vol. 15, no. 14, pp. 3065–3090, 2021.

[2] J. V. Ringwood, G. Bacelli, and F. Fusco, "Energy-maximizing control of wave-energy converters: The development of control system technology to optimize their operation," *IEEE Control Syst.*, vol. 34, no. 5, pp. 30–55, Oct. 2014.

[3] N. Faedo, D. García-Violini, Y. Peña-Sanchez, and J. V. Ringwood, "Optimisation-vs. non-optimisation-based energy-maximising control for wave energy converters: A case study," in *Proc. IEEE Eur. Control Conf.*, 2020, pp. 843–848.

[4] N. Faedo, S. Olaya, and J. V. Ringwood, "Optimal control, MPC and MPC-like algorithms for wave energy systems: An overview," *IFAC J. Syst. Control*, vol. 1, pp. 37–56, 2017.
[5] G. Bacelli and J. V. Ringwood, "Numerical optimal control of wave energy converters," *IEEE Trans. Sustain. Energy*, vol. 6, no. 2, pp. 294–302, Apr. 2015.
[6] N. Faedo, G. Scarciotti, A. Astolfi, and J. V. Ringwood, "Energy-maximising control of wave energy converters using a moment-domain representation," *Control Eng. Pract.*, vol. 81, pp. 85–96, 2018.
[7] D. García-Violini, N. Faedo, F. Jaramillo-Lopez, and J. V. Ringwood, "Simple controllers for wave energy devices compared," *J. Mar. Sci. Eng.*, vol. 8, no. 10, 2020, Art. no. 793.
[8] F. Fusco and J. V. Ringwood, "A simple and effective real-time controller for wave energy converters," *IEEE Trans. Sustain. Energy*, vol. 4, no. 1, pp. 21–30, Jan. 2013.
[9] D. García-Violini, Y. Peña-Sanchez, N. Faedo, C. Windt, F. Ferri, and J. V. Ringwood, "Experimental implementation and validation of a broadband LTI energy-maximizing control strategy for the wavestar device," *IEEE Trans. Control Syst. Technol.*, vol. 29, no. 6, pp. 2609–2621, Nov. 2021.
[10] D. García-Violini, Y. Pena-Sanchez, N. Faedo, C. Windt, and J. V. Ringwood, "LTI energy-maximising control for the wave star wave energy converter: Identification, design, and implementation," *IFAC-PapersOnLine*, vol. 53, no. 2, pp. 12313–12318, 2020.
[11] N. E. Huang et al., "The empirical mode decomposition and the hilbert spectrum for nonlinear and non-stationary time series analysis," *Proc. Roy. Soc. London. Ser. A: Math. Phys. Eng. Sci.*, vol. 454, no. 1971, pp. 903–995, 1998.
[12] J. Falnes, *Ocean Waves and Oscillating Systems: Linear Interactions Including Wave-Energy Extraction*. Cambridge, U.K.: Cambridge Univ. Press, 2002.
[13] W. E. Cummins, "The impulse response function and ship motions," *Schiffstechnik*, vol. 47, pp. 101–109, 1962.
[14] T. F. Ogilvie, "Recent progress toward the understanding and prediction of ship motions," in *Proc. 5th Symp. Nav. Hydrodynamics*, Bergen, Norway, 1964, vol. 1, pp. 2–5.
[15] Wamit Inc, WAMIT UserManual, Accessed: Aug. 1, 2019. [Online]. Available: http://tinyw.in/7u4T, 2019.
[16] N. Faedo, Y. Peña-Sanchez, and J. V. Ringwood, "Finite-order hydrodynamic model determination for wave energy applications using moment-matching," *Ocean Eng.*, vol. 163, pp. 251–263, 2018.
[17] P. B. Garcia-Rosa, G. Kulia, J. V. Ringwood, and M. Molinas, "Real-time passive control of wave energy converters using the hilbert-huang transform," *IFAC-PapersOnLine*, vol. 50, no. 1, pp. 14705–14710, 2017.
[18] M. Garcia-Abril, F. Paparella, and J. V. Ringwood, "Excitation force estimation and forecasting for wave energy applications," *Proc. IFAC-PapersOnLine*, vol. 50, pp. 14692–14697, 2017.
[19] P. V. Overschee and B. De Moor, *Subspace Identification for Linear Systems - Theory Implication Applications*. Berlin, Germany: Springer, 1996.
[20] K. Hasselmann, "Measurements of wind wave growth and swell decay during the joint north sea wave project (JONSWAP)," *Deutches Hydrographisches Inst.*, vol. 8, p. 95, 1973.

Demián García-Violini received the B.S. degree in automation and control engineering from the National University of Quilmes (UNQ), Bernal, Argentina, in 2010, and the Doctoral degree in engineering from the Buenos Aires Institute of Technology, Buenos Aires, Argentina, in 2015. He is currently a Researcher with the Department of Science and Technology, UNQ, and CONICET, Argentina. He is also with the Centre for Ocean Energy Research, Maynooth University, Ireland. His research interests include control and system ID in wave energy systems, and biomedical engineering. He currently serves as Guest Editor of the IEEE LATIN AMERICA TRANSACTIONS

Yerai Peña-Sanchez received the Degree in renewable energy engineering from the University of the Basque Country, Leioa, Spain, in 2016, and the Ph.D. degree from the Centre for Ocean Energy Research (COER) from NUI Maynooth, Ireland, in 2020, which focused on wave excitation force estimation and forecasting for wave energy applications. He was a Postdoctoral for a year with COER designing and building two hardware-in-the-loop systems to test optimal control and estimation strategies for wave energy converters. He is currently holds a Postdoctoral position with EHU as a recipient of the cofunded Marie Skłodowska-Curie Fellowship, where he works on fault detection and fault tolerant control for offshore wind farms.

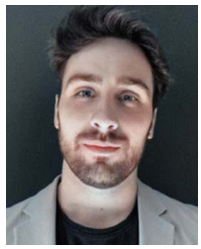

Nicolás Faedo was born in Buenos Aires, Argentina, in 1991. He received the Degree in automation and control engineering from the National University of Quilmes, Bernal, Argentina, in 2015, and the Ph.D. degree in electronic engineering from the Centre for Ocean Energy Research group, Maynooth University, Ireland, in 2020, with a focus on optimal control and model reduction for wave energy converters from a system-theoretic perspective. He is currently holds a Postdoctoral position with the Department of Mechanical and Aerospace Engineering, Politecnico di Torino, Turin, Italy, and was the recipient of the Marie Skłodowska-Curie Actions Individual Fellowship (MSCA-IF 2020).

Francesco Ferri received the master's degree in chemical and process engineering from the University of Bologna, Bologna, Italy, in 2008, and the Ph.D. degree in experimental and numerical modelling of wave energy converters from Aalborg University, Aalborg, Denmark. His research interests include hydrodynamic interaction in renewable energy offshore parks and control of wave energy converters.

John V. Ringwood (Senior Member, IEEE) received the Diploma degree in electrical engineering from the Dublin Institute of Technology, Dublin, Ireland, in 1981, and the Ph.D. degree in control systems from the University of Strathclyde, Glasgow, U.K., in 1985. He is currently a Professor of electronic engineering and the Director of the Centre for Ocean Energy Research with Maynooth University, Ireland. He is also a Chartered Engineer and a Fellow of the Institution of Engineers of Ireland. His research interests include time series modelling, wave energy, and biomedical engineering. He is on the Editorial boards of the *Journal of Ocean Engineering and Marine Energy*, IEEE TRANSACTIONS ON SUSTAINABLE ENERGY, and *IET Renewable Power Generation*.